# Microwave Irradiation of Alkali-activated Metakaolin Slurry

Barbara Horvat, Branka Mušič, Majda Pavlin, Vilma Ducman

Slovenian National Building and Civil Engineering Institute, Ljubljana, Slovenia
barbara.horvat@zag.si, branka.music@zag.si, majda.pavlin@zag.si, vilma.ducman@zag.si

**Abstract** The building and civil engineering industry generates more than 40% of man-caused carbon emissions, consumes a lot of energy just to produce building materials, generates a large amount of waste through construction and demolition, and consumes a large amount of natural resources. One of the possible solutions is to use alkali-activated materials, which can use waste instead of raw materials and are produced at lower temperatures, with less energy consumption and in less time than traditional building products. All of this lowers the carbon footprint, which could be further reduced by the timely-short implementation of microwave irradiation in the early stages of alkali-activation synthesis. Therefore, metakaolin activated with Na-water glass in a theoretically optimal ratio was irradiated with microwaves of 2.45 GHz at powers of 100 W and 1000 W for 1 min, and compared to non-irradiated reference cured only at room conditions. Samples prepared at higher power, i.e., 1000 W, solidified completely and foamed. TG-DTA was performed on all samples in the early stages of curing, mechanical strengths were measured on 3 and 28-day-old samples, and leaching tests on aged samples.

**Keywords:** alkali-activation, metakaolin, microwaves, TG/DTA, mechanical strengths

University of Maribor Press

DOI https://doi.org/10.18690/um.fkkt.1.2023.2
ISBN 978-961-286-692-1

## 1 Introduction

Alkali-activated materials (AAMs) are made from solid pulverized precursors containing a significant amount of amorphous Si and Al "activated" by alkali (hydroxides or/and silicate solution) (Provis, 2013). The process of alkali-activation starts with the dissolution of the precursor in the alkali liquid, rearrangement of the dissolved components into monomers with help of diffusion, followed by the "coagulation" of the monomers into the dehydrated polymer (Marvila et al., 2021; Pacheco-Torgal et al., 2008). This inorganic polymer consists of $SiO_2$ and $AlO_2^{1-}$ tetrahedra connected through O-bridges, where the $1^-$ charge of Al is compensated by ions of the 1st and 2nd group of the periodic system (Škvára, 2007). The formed aluminosilicate network (ASN) is usually and mainly amorphous, and when the precursor used is metakaolin, the AAM can also be called a geopolymer (Ameri et al., 2019).

If compact ASN is foamed, AAM becomes alkali-activated foam (AAF), i.e., a lightweight material with lower geometric density, lower mechanical strength, but higher acoustic and/or thermal insulation ability. The foaming process can be mechanical (Hajimohammadi et al., 2017a), chemical (Burkhard Walther et al., 2017; Hajimohammadi et al., 2017b) and/or physical (Fletcher et al., 2005; Horvat and Ducman, 2020a; Rincón Romero et al., 2019; Wei et al., 2016). The mechanical introduction of the pores into the alkali-activated slurry of proper viscosity (not too low, otherwise bubbles would escape, and not too high, since reaching a uniform distribution of the pores could not be achieved) is done by mechanical mixing of the pre-prepared foam with the freshly alkali-activated slurry, in which the chemical reactions are still in progress. Chemical foaming (Horvat and Ducman, 2019) is performed by adding foaming agents (e.g., liquid $H_2O_2$, solid Na-perborate, solid pulverized Al) and stabilizing agents (e.g., liquid triton, solid soybean lecithin, solid Na-oleate, solid Na-dodecyl sulphate) to the solid pulverized precursor or to the liquid alkali. Solid ingredients are mixed with the solid precursor and liquid ingredients are mixed with the liquid alkali to avoid premature reactions and loss of bubbles. Homogenized solids and homogenized liquids are mixed as briefly as necessary to ensure wetting of the components and uniform distribution of all reagents. Besides induced chemical foaming, self-foaming (Horvat and Ducman, 2020b) may occur if the precursor contains substances that react with alkali(s) with

the release of gasses into the slurry, ending as alkali-activated self-foam (AAsF). Foaming reactions can be immediate (AAF) or delayed (AAdF), as also some precursors require less time for curing (metakaolin, slags) and others more (fly-ash, mineral wools) if curing is performed under room conditions. If the curing temperature is increased, the curing time is reduced (Horvat and Ducman, 2019) and the release of bubbles out from the slurry is hindered.

In this work, the influence of irradiation with microwaves of different power on alkali-activated metakaolin slurry in its early stages was studied. Metakaolin was used for alkali-activation because this material is widely used in alkali-activated research.

## 2 Method

For chemical (X-ray fluorescence, XRF; Thermo Scientific ARL Perform'X Sequential XRF) and mineralogical (X-ray powder diffraction, XRD; Empyrean PANalytical X-ray Diffractometer, Cu X-Ray source) analysis of metakaolin (MK), the precursor was dried, milled and sieved below 125 μm.

XRF measurement was performed on molten discs and analysed using UniQuant 5. The XRD diffractogram was solved using X'Pert Highscore plus 4.1. Rietveld refinement was performed with an external standard (corundum, $Al_2O_3$) to estimate the amount of amorphous content and minerals.

From the XRF and XRD results, the amounts of Si, Al and 1st group of the periodic system were determined as described in our previous work (Horvat and Ducman, 2019). The amount of substance of precursor and added alkali (Na-silicate solution, Geosil, 344/7, Woelner, Ludwigshafen, Germany, 16.9% $Na_2O$, 27.5% $SiO_2$) for Si, Al, Na was aimed to be 1.9, 1, "≤1", respectively, to achieve the highest possible compressive strength and avoid efflorescence (Duxson et al., 2005). The theoretically determined mass ratio between precursor and Na-silicate solution was 1:0.66, respectively.

After mixing MK with alkali until the slurry was completely wetted, the slurry was moulded into moulds made of silicone-urethane rubber. Reference was cured exclusively under room conditions, while the others were irradiated with microwaves

of frequency 2.45 GHz, with power of 100 W and 1000 W, for 1 min, not-covered and covered with another silicone-urethane rubber mould to avoid rapid dehydration while the sample was being irradiated. The inverter type microwave (Panasonic, NN-CD575M) was used, i.e., the microwaves work constantly, unlike an ordinary kitchen microwave where the microwaves work for a short period of time, then turn off and repeat the cycle.

The mechanical strengths (bending and compressive) of the AAMs were measured with a compressive and bending strength testing machine (ToniTechnik ToniNORM) 3 and 28 days after moulding.

Thermogravimetric analysis and differential thermal analysis (TG/DTA; STA 409 PC Luxx, Netzsch, Germany) were performed on all samples 12 min after mixing the ingredients and compared with the non-irradiated sample more than 1-year-old. Fresh samples were followed to constant mass. Samples of about 40 mg were heated in airflow from room temperature to 1000 °C at a rate of 10 K/min to evaluate the mass changes (mainly water losses) as a function of temperature.

Moisture of the 3 and 28-day-old samples was determined by mass loss using an IR moisture analyser (Mettler Toledo, HE73).

Evaluation of the presence of toxic elements in leachates was performed on 28-day-old samples according to the European standard SIST EN 12457-2. AAM/AAF was crushed to grain sizes lower than 4 mm and added into deionised water in a glass bottle with solid:liquid mass ratio of 1:10, respectively. Suspensions were rotated around the vertical axis for 24 h at room conditions, then filtered below 0.45 μm. The obtained liquid fraction was acidified to pH<2 with $HNO_3$ for determination of the amount of released metals by inductively coupled plasma mass spectrometer (ICP-MS, Agilent 7900). Results were compared to the total amount of toxic trace and minor elements measured in the precursor and with the legislation (Decre on waste landfill).

## 3 Results

Chemical analysis (XRF) of MK is shown in Table 1. Regarding the potential for use as a precursor in alkali-activation, MK contains a significant amount of $SiO_2$ and $Al_2O_3$ needed for ASN formation, while elements of the 1st and 2nd group are scarce, allowing the possibility of adding more alkali and still avoiding efflorescence.

**Table 1: Oxides with mass percent (m%) above 0.1% present in MK according to XRF analysis.**

| Oxides [m%] | $Na_2O$ | $K_2O$ | MgO | CaO | $Al_2O_3$ | $SiO_2$ | $TiO_2$ | $Fe_2O_3$ |
|---|---|---|---|---|---|---|---|---|
| XRF | 0.29 | 0.18 | 0.17 | 0.48 | 25.58 | 69.46 | 1.13 | 2.32 |

The XRD diffractogram of MK (Figure 1, black line) shows the presence of the amorphous content (the amorphous halo has 2θ peak around 25°, indicating that the Si:Al ratio is above 2:1 (Tokoro et al., 2014), which is consistent with the XRF results in Table 1) and minerals, where quartz represents the majority. Mineralogical analysis of MK with Rietveld refinement, presented in Table 2, shows more than 60% of the amorphous content and more than 30% of quartz.

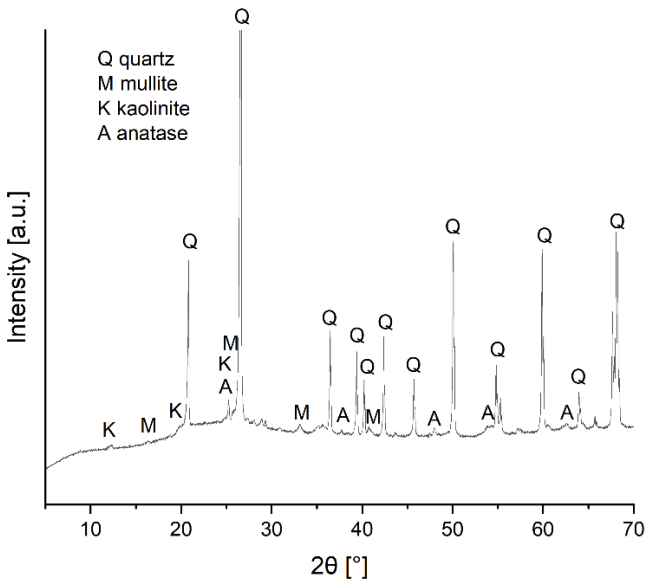


**Figure 1. XRD pattern of MK.**

Source: own.

**Table 2. Minerals in mass percent (m%) present in MK according to Rietveld refinement analysis on XRD pattern.**

| Minerals [m%] | Quartz | Mullite | Kaolinite | Anatase | Amorphous content |
|---|---|---|---|---|---|
| XRD | 33.5 | 3.3 | 1.1 | 0.5 | 61.6 |

The XRF (Table 1) and XRD (Table 2) results were recalculated onto elements to estimate the amount of amorphous content per element (Table 3) (Horvat and Ducman, 2019).

**Table 3. Mass percentage of elements in the amorphous content.**

| Elements [m%] | Na | K | Mg | Ca | Al | Si |
|---|---|---|---|---|---|---|
| XRF-XRD | 0.21 | 0.15 | 0.10 | 0.35 | 11.96 | 16.21 |

The amount of amorphous content of Si:Al in the mixture of MK and Na-silicate solution together was aimed to be 1.9:1, respectively. The mass ratio of MK and Na-silicate solution, 1:0.66, resulted in the amount of substance ratios Si:Al:1st group:2nd group=1.99:1:0.84:0.03. If not all (amorphous) Al dissolves, efflorescence still might not occur, since the initial amount of substance of alkali ions is below Al.

The visual results of alkali-activation are shown in Figure 2. Irradiation of freshly moulded alkali-activated MK slurry with microwaves at 100 W for 1 min (Figure 2, (b) samples 2 and 3) resulted in AAM looking like non-irradiated AAM (Figure 2, (b), sample 1). While irradiation with microwaves at 1000 W for 1 min caused alkali-activated slurry to foam (Figure 2, (b), samples 4 and 5) and the material hardened completely, which was in comparison with other samples very hot immediately after irradiation. If the mould was sealed when the slurry was irradiated at 1000 W (Figure 2, (c), samples 5 and 6), and if the slurry "touched" the cover during foaming (Figure 2, (c), sample 6), it began to damage material's framework from above. This can be seen on the top surface in Figure 2, (c), sample 6, and its' side surface in Figure 2, (d).

The thermal behaviour of the samples was determined by TG/DTA, and is shown in Figure 3, Figure 4 and Table 4: 1-year-old non-irradiated sample (red), fresh non-irradiated sample (orange), irradiated sample at 100 W for 1 min (light blue), irradiated sample at 100 W for 1 min and covered during microwave irradiation (dark

blue), irradiated sample at 1000 W for 1 min (light pink), and irradiated sample at 1000 W for 1 min and covered during microwave irradiation (dark pink).

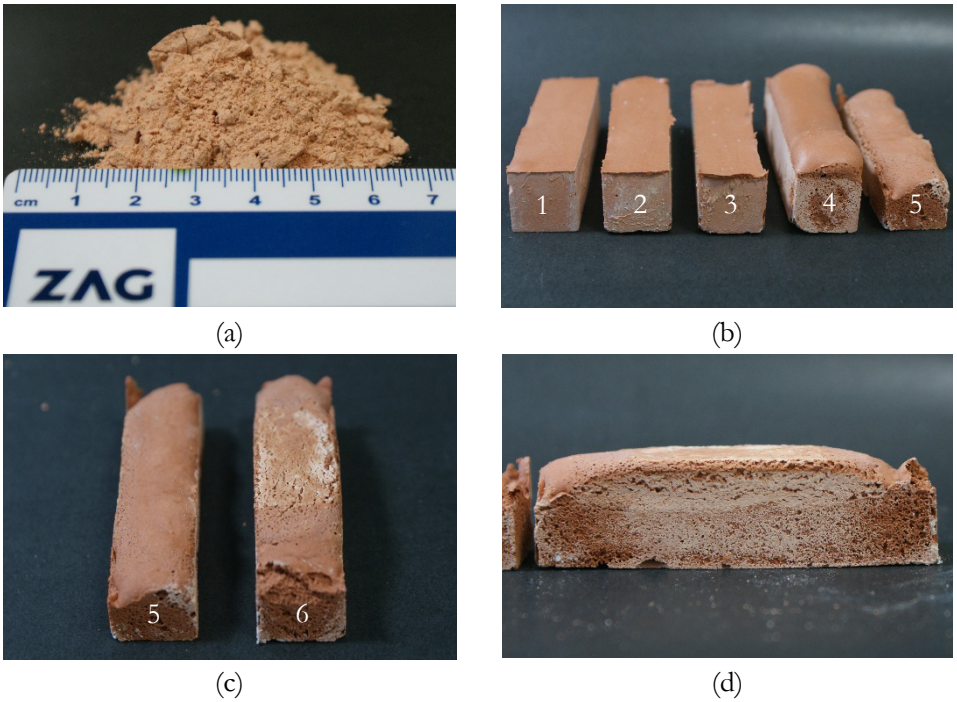


(a) (b)

(c) (d)

**Figure 2: Photography of (a) MK and its (b) alkali-activated counterparts (cured at 1) room conditions, 2) and 3) at 100 W for 1 min in 2) open and 3) closed mould, 4) and 5) at 1000 W for 1 min in 4) open and 5) closed mould). (c) Alkali-activated MK cured for 1 min at 1000 W in the closed mould where prism 5) did not reach the cover, 6) and (d) reached the cover of the mould during "foaming".**

Source: own.

$H_2O$ in the initial slurry was mainly from Na-water glass and accounted for 20.9% of the combined mass of precursor and Na-water glass. The measured moisture of MK was 0.5%, indicating that the initial amount of water in the slurry (corrected for the moisture in the precursor) was approximately 21.0%.

Total mass losses were about 13.7% for the 1-year-old non-irradiated sample and 21.5% for the fresh, non-irradiated and not-hardened sample. About 21.1% for the sample irradiated at 100 W for 1 min and similarly for the covered sample, i.e., the total mass loss was about 21.3%. For non-irradiated and the 100 W irradiated samples, the total mass loss a slightly less than the total "theoretical" initial amount of water (which could be due to the human error in weighing the ingredients or/and to degradation of compounds present in "trace" amounts in the slurry and in AAM/AAF). Therefore, irradiation for 1 min at 100 W had no effect on dehydration and crack-pore formation.

The total mass loss of the sample irradiated at 1000 W for 1 min was about 11.4% and very similar results were obtained for the covered alternative, i.e., the mass loss was about 13.6%, as shown in Figure 3. This value is comparable to the mass loss of the non-irradiated aged sample, leading to the conclusion that the slurry irradiated with higher microwave power completed the long-term aging process in only 1 min. This was possible only in the case of extreme dehydration accompanied by pore-formation (Figure 2).

In both cases of covered/uncovered samples, i.e., irradiated at 100 W and 1000 W, the mass loss was higher for the covered samples, which is attributed to the retention of water in the covered sample during microwave irradiation and the successful hindering of dehydration. While synthesis in covered moulds can be described as hydrothermal synthesis at lower pressure (and with the possibility of release depressurizing by lifting the cover when the pressure reaches 235 Pa), cooking, synthesis in open moulds can be described as "baking".

The TG curves show that significant mass losses occur in two temperature ranges, (i) from room temperature to 200 °C due to the evaporation of free water adsorbed on the surface, as well as the retained water trapped in the pores of the sample, and some chemically bonded water, and (ii) between 200 °C and 600 °C, where mass losses range from 1.1% to 2.7%. In this temperature range, the mass loss is mainly due to evaporation of retained chemically bound water and dehydroxylation of unreacted kaolinite, which occurs between 400 °C and 600 °C (Alshaaer et al., 2016) and vary between 0.2 and 1%. Samples irradiated at 1000 W had lower mass losses in this range, indicating that irradiation already affected compounds decomposing in

the 200 °C to 600 °C range. Lower mass losses were again for samples irradiated at 1000 W, indicating that the irradiation most likely affected the crystal structure of the kaolinite and made it available for the alkali-activated reaction. Lower mass losses from about 700 °C could be due to $CO_2$ losses from calcite (Frost et al., 2009), which, interestingly, are significantly higher in both cases of irradiation at 1000 W, i.e., covered and not covered, as shown in Table 4. This means that the small amount of Ca present in MK contributes in ASN, onlly that it did not have enough time to dissolve in less than 1 min of high-power microwave irradiation.

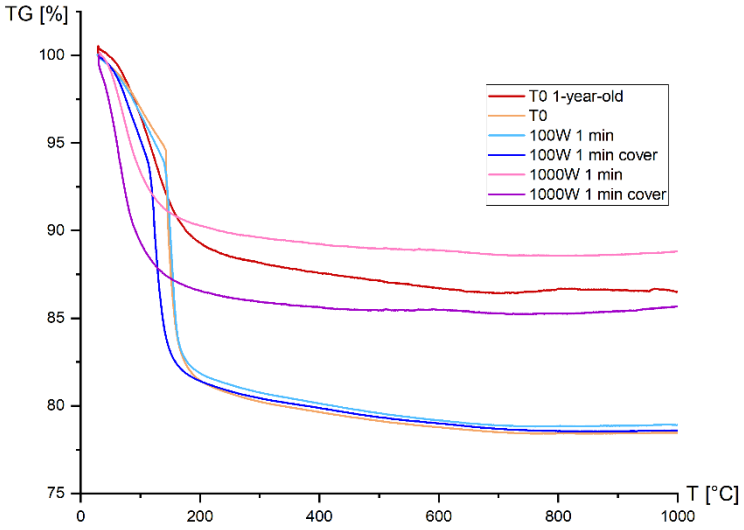


**Figure 3: TG of alkali-activated samples: 1-year-old non-irradiated sample (red), fresh non-irradiated sample (orange), sample irradiated at 100 W for 1 min (light blue), its covered alternative (dark blue), sample irradiated at 1000 W for 1 min (light pink), and its covered alternative (dark pink).**

Source: own.

Figure 4 shows the DTA curves. The fresh, non-irradiated sample and the sample irradiated at 100 W for 1 min (orange and light blue curves, respectively), which have the largest mass loss up to 200 °C, also have the narrowest and most pronounced course of the curve. They are followed by the sample irradiated at 100 W for 1 min while covered (dark blue curve) and then the sample irradiated at 1000 W for 1 min (dark pink curve), which was also covered during microwave irradiation. The 1-year-old non-irradiated sample (red curve) and the sample irradiated at 1000 W for 1 min

(light pink curve), which show the lowest mass loss in the temperature range up to 200 °C, have a broad curve shape and the least endothermic peak. The curve shape of a one-year-old sample differs from freshly prepared samples, which have a much larger and narrower endothermic curve. The differences are due to the fact that 1-year-old sample does not contain as much free adsorbed water and the peak is smaller due to the smaller amounts of adsorbed water. The boader endothermic course of the curve is due to the presence of interstitial and bound water, which is released at higher temperatures than the free adsorbed water. Also, the not-covered sample irradiated at 1000 W for 1 min shows a lower peak, which is due to dehydration during microwave irradiation. The adsorbed water content in this sample is also lower than in the others, as can be seen from the TG curves in Figure 3 and Table 4.

**Table 4: Total mass loss and mass loss over different temperature ranges.**

| Samples | Total mass loss [%] | Mass loss over different temperature ranges | | | |
|---|---|---|---|---|---|
| | | T0-200 °C [%] | 200-600 °C [%] | 400-600 °C [%] | > 700 °C [%] |
| T0 1-year-old | 13.8 | 11.1 | 2.6 | 0.9 | 0.1 |
| T0 | 21.4 | 18.4 | 2.7 | 0.9 | 0.04 |
| 100 W 1 min | 20.9 | 18.0 | 2.7 | 1.0 | 0.03 |
| 100 W 1 min covered | 21.3 | 18.5 | 2.4 | 0.9 | 0.1 |
| 1000 W 1 min | 11.4 | 9.9 | 1.4 | 0.4 | 0.2 |
| 1000 W 1 min covered | 13.6 | 12.7 | 1.1 | 0.2 | 0.4 |

All samples also show a small endothermic peak just before 600 °C, which is attributed to the endothermic dehydroxylation reaction, which, according to the literature, occurs somewhere between 530 and 590 °C (Deju et al., n.d.).

Moisture (Table 5) in the alkali-activated samples was highest in sample cured only at room conditions, while the other samples had less moisture, but not more than 4% less when 3 days old and not less than 1.5% when 8 days old. Comparing the TG mass loss in the range of room temperature to 200 °C for a 1-year-old sample (Table 4) and its moisture content (Table 5), there could be about 4.5% chemically bound water. Dehydration of the slurries at room temperature is most pronounced in the samples prepared without irradiation and samples irradiated with microwaves of 100 W. The difference between the TG mass loss in the range between T0 and 200 °C (Table 4) and the measurement of moisture after 3 days (Table 5) is between

5% and 6% for the mentioned samples, while for the samples irradiated at 1000 W this difference is less significant. However, dehydration continues and the amount of moisture in all samples after 28 days is comparable to or close to the final equilibrium for samples left at room conditions.

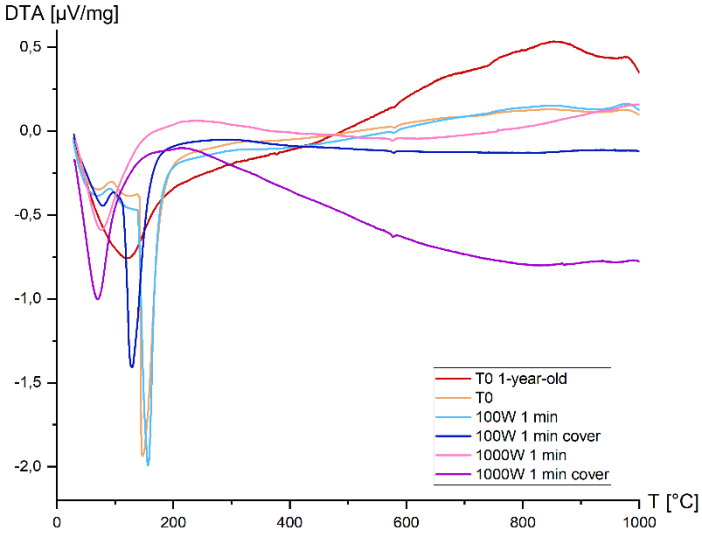


**Figure 4: DTA of alkali-activated samples: 1-year-old non-irradiated sample (red), fresh non-irradiated sample (orange), sample irradiated at 100 W for 1 min (light blue), its covered alternative (dark blue), sample irradiated at 1000 W for 1 min (light pink), and its covered alternative (dark pink).**

Source: own.

**Table 5. Moisture in 3-day-old and 28-day-old alkali-activated samples was determined by IR heating at 105 °C.**

| Sample | T0 | 100 W 1 min | 100 W 1 min covered | 1000 W 1 min | 1000 W 1 min covered |
|---|---|---|---|---|---|
| **Moisture 3 days [%]** | 13.5 | 11.8 | 12.0 | 9.7 | 13.1 |
| **Moisture 28 days [%]** | 7.8 | 6.7 | 7.1 | 6.5 | 7.5 |
| **Moisture 1-year-old [%]** | 6.6 | / | / | / | / |

Compressive and bending strengths, the most important parameters for structure-functional products in building and civil engineering, are shown in Figure 5 and Table 6. For all three AAMs (sample prepared at room temperature, and both

samples irradiated at 100 W), geometric densities are identical, but the compressive strengths differ significantly. However, after 28 days, all samples reach comparable values of mechanical strengths, while thee geometric densities decrease uniformly for all of them. The conclusion is that low-power microwave irradiation enhanced the early reactions (dissolution, diffusion, self-assembly, i.e., networking-gelation of ASN) and curing without affecting dehydration. The final internal chemistry of ASN probably did not change, as did the porosity and amount of ASN.

For foamed samples, as expected, a large decrease in geometric densities of both AAFs (samples irradiated at 1000 W) resulted in a large decrease in early compressive strength. AAF prepared in closed mould exhibited lower compressive and bending strengths, most likely due to the of pore structure and ASN framework collapsing under the pressure of the limited space for material expansion during foaming (Figure 2, (c) and (d)). With time, the mechanical strengths increased, but the compressive strength reached only approximately 15% of the highest compressive strength of the 28-day-old AAM.

The relative error of the early measurement of mechanical strengths (standard deviation) increased with microwave power. This increase in comparison with AAM, which was prepared exclusively under room conditions, is a consequence of the non-uniform distribution of microwaves in the microwave. The reason for the huge increase in the relative error of the AAFs was mainly a consequence of the large decrease in mechanical strengths. With time, the absolute error of the compressive strength of the AAMs increased, which means that the samples need more time to reach the final values of mechanical strength.

The effect of microwave irradiation on the immobilization of trace and minor elements was tested by leaching experiments and the results are shown in Table 7. The concentrations of the elements are compared with the legislation values specified in the Decree on Waste Landfills. For the leaching experiments, the leaching of precursor (MK) and AAMs was performed. MK shows concentrations of all elements below the inert waste limit. However, for the AAMs, the activation process was found to increase the leaching potential for Cr, Ni, Cu, and As, while the concentrations of the other elements were comparable to those of the precursor. In addition, the concentrations of AAMs for Cr and As exceeded the limits for inert

(As in samples prepared at 100 W and Cr in samples prepared at 1000 W) and in some cases even for non-hazardous waste (As in samples prepared at 1000 W). This suggests that microwave irradiation accelerates the leaching of As and Cr when exposed to high working power. However, for As and Cr, we did not observe any difference when the samples were cured at room temperature or irradiated at 100 W.

**Table 6: Compressive and bending strength, their absolute and relative error, and geometric density of 3-days-old and 28-days-old alkali-activated samples.**

| 3-days-old samples | CS [MPa] | $\sigma_{CS}$ [MPa] | $\sigma_{CS}$ [%] | BS [MPa] | $\sigma_{BS}$ [MPa] | $\sigma_{BS}$ [%] | $\varrho$ [kg/dm$^3$] |
|---|---|---|---|---|---|---|---|
| **T0** | 34.9 | 5.0 | 14.2 | 7.6 | 0.3 | 4.2 | 1.9 |
| **100 W 1 min** | 51.6 | 8.5 | 16.5 | 7.8 | 0.7 | 8.5 | 1.9 |
| **100 W 1 min cover** | 64.8 | 2.5 | 3.9 | 8.2 | 0.8 | 10.0 | 1.9 |
| **1000 W 1 min** | 9.1 | 2.5 | 27.5 | 4.0 | 0.9 | 23.7 | 1.2 |
| **1000 W 1 min cover** | 2.1 | 0.8 | 32.4 | 2.0 | 0.3 | 17.2 | 1.0 |
| 28-days-old samples | CS [MPa] | $\sigma_{CS}$ [MPa] | $\sigma_{CS}$ [%] | BS [MPa] | $\sigma_{BS}$ [MPa] | $\sigma_{BS}$ [%] | $\varrho$ [kg/dm$^3$] |
| **T0** | 66.0 | 13.4 | 20.4 | 9.1 | 0.6 | 7.1 | 1.7 |
| **100 W 1 min** | 67.8 | 12.0 | 17.7 | 10.5 | 0.8 | 7.3 | 1.7 |
| **100 W 1 min cover** | 66.8 | 11.6 | 17.4 | 10.1 | 0.1 | 1.1 | 1.8 |
| **1000 W 1 min** | 11.9 | 7.1 | 59.6 | 6.6 | 2.6 | 38.6 | 1.2 |
| **1000 W 1 min cover** | 9.2 | 1.7 | 18.3 | 3.6 | 0.4 | 10.3 | 1.0 |

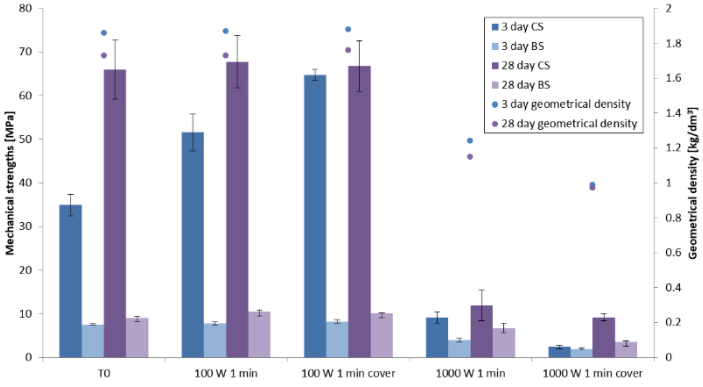


**Figure 5: Compressive (CS) and bending (BS) strengths with geometric densities of 3-days-old and 28-days-old alkali-activated samples.**

Source: own.

**Table 7: The concentrations in mg/kg of selected elements were measured in the digested samples and leachates according to SIST EN:12457-2 standard protocol.**

| Element [mg/kg] | Cr | Ni | Cu | Zn | As | Se | Mo | Cd | Sb | Ba | Hg | Pb |
|---|---|---|---|---|---|---|---|---|---|---|---|---|
| MK | 0.22 | 0.0004 | 0.0008 | 0.004 | 0.08 | 0.06 | 0.02 | <0.002 | 0.002 | 0.02 | <0.001 | 0.0001 |
| AAM T0 | 0.20 | 0.03 | 0.03 | 0.010 | 0.62 | 0.03 | 0.03 | <0.002 | 0.003 | 0.003 | 0.003 | 0.005 |
| AAM 100 W 1 min | 0.17 | 0.02 | 0.03 | 0.007 | 0.57 | 0.03 | 0.02 | <0.002 | 0.002 | 0.004 | 0.002 | 0.005 |
| AAM 1000 W 1 min | 0.97 | 0.02 | 0.02 | 0.005 | 2.66 | 0.08 | 0.07 | <0.002 | 0.006 | 0.003 | 0.002 | 0.002 |
| ***Inert waste**** | 0.5 | 0.4 | 2.0 | 4.0 | 0.5 | 0.1 | 0.5 | 0.04 | 0.06 | 20.0 | 0.01 | 0.5 |
| ***Non-hazardous waste**** | 10.0 | 10.0 | 50.0 | 50.0 | 2.0 | 0.5 | 10.0 | 3 | 0.7 | 100.0 | 0.20 | 10.0 |

*Decree on waste landfill: http://www.pisrs.si/Pis.web/pregledPredpisa?id=URED6660#

## 4 Conclusion

When microwave irradiation of sufficiently high power was used in the very early stages of alkali-activated slurry curing, the alkali-activation process ended in a very short time as alkali-activated foam. At lower microwave powers, the alkali-activated samples ended up as non-foamed alkali-activated materials with much higher early mechanical strengths compared to the non-irradiated reference, but the curing time was not shortened, i.e., the microwaves only enhanced early-stage dissolution in alkali-activated synthesis.

From the thermogravimetric analysis, it is evident that the power of microwave irradiation has a significant effect on the course of the curves. Differences are also observed between uncovered samples during microwave irradiation and covered samples during microwave irradiation, which complicates the evaporation of water during irradiation. The 1-year-old sample was found to be most similar to the sample irradiated at 1000 W for 1 min. TG/DTA analysis showed that microwave irradiation at lower microwave powers (100 W) for 1 min did not result in significant differences compared to the non-irradiated samples.

Alkali-activation did show an increase in leaching of As, low powers of irradiation with microwaves did not have additional influence on it, while high irradiation powers additionally increased leaching of As and Cr.

Concentrations for most of the toxic trace and minor elements were low except for As and Cr. Cr exceeded the limit for inert waste when alkali-activated slurries were irradiated at 1000 W, whereas As exceeded values for inert waste for all AAMs. Moreover, in the case of samples irradiated at 1000 W, Cr exceeded the values also for non-hazardous waste. Research showed that irradiation at higher working power decreased the immobilization potential of As, i.e. microwaves shows potential to remove heavy elements from dangerous materials and thus could present efficient method for recovery or remediation.

**Acknowledgement**

This work is part of the ARRS project of dr. Barbara Horvat and was financially supported by the Slovenian Research Agency under Grant no. J2-3035.

This work is part of the postdoc project of dr. Majda Pavlin and was financially supported by the Slovenian Research Agency under Grant no. Z2-3199.

**References**

Alshaaer, M., El-Eswed, B., Yousef, R.I., Khalili, F., Rahier, H., 2016. Development of functional geopolymers for water purification, and construction purposes. Journal of Saudi Chemical Society 20, S85–S92. https://doi.org/10.1016/j.jscs.2012.09.012

Ameri, F., Shoaei, P., Zareei, S.A., Behforouz, B., 2019. Geopolymers vs. alkali-activated materials (AAMs): A comparative study on durability, microstructure, and resistance to elevated temperatures of lightweight mortars. Construction and Building Materials 222, 49–63. https://doi.org/10.1016/j.conbuildmat.2019.06.079

Burkhard Walther, Bernhard Feichtenschlager, Shengzhong Zhou, 2017. Self-foaming Geopolymer Composition COntaining Aluminum Dross. US 9,580,356 B2.

Deju, R., Cucos, A., Mincu, M., Tuca, C., n.d. Thermal characterization of kaolinitic clay 8.

Duxson, P., Provis, J.L., Lukey, G.C., Mallicoat, S.W., Kriven, W.M., van Deventer, J.S.J., 2005. Understanding the relationship between geopolymer composition, microstructure and mechanical properties. Colloids and Surfaces A: Physicochemical and Engineering Aspects 269, 47–58. https://doi.org/10.1016/j.colsurfa.2005.06.060

Fletcher, R.A., MacKenzie, K.J.D., Nicholson, C.L., Shimada, S., 2005. The composition range of aluminosilicate geopolymers. Journal of the European Ceramic Society 25, 1471–1477. https://doi.org/10.1016/j.jeurceramsoc.2004.06.001

Frost, R.L., Hales, M.C., Martens, W.N., 2009. Thermogravimetric analysis of selected group (II) carbonateminerals — Implication for the geosequestration of greenhouse gases. J Therm Anal Calorim 95, 999–1005. https://doi.org/10.1007/s10973-008-9196-7

Hajimohammadi, A., Ngo, T., Mendis, P., Kashani, A., van Deventer, J.S.J., 2017a. Alkali activated slag foams: The effect of the alkali reaction on foam characteristics. Journal of Cleaner Production 147, 330–339. https://doi.org/10.1016/j.jclepro.2017.01.134

Hajimohammadi, A., Ngo, T., Mendis, P., Sanjayan, J., 2017b. Regulating the chemical foaming reaction to control the porosity of geopolymer foams. Materials & Design 120, 255–265. https://doi.org/10.1016/j.matdes.2017.02.026

Horvat, B., Ducman, V., 2020a. Influence of curing/drying methods including microwave heating on alkali activation of waste casting cores, in: COMS 2020. Presented at the 2nd International Conference on Construction Materials for Sustainable Future, Bled, Slovenia.

Horvat, B., Ducman, V., 2020b. Influence of Particle Size on Compressive Strength of Alkali Activated Refractory Materials. Materials 13, 2227. https://doi.org/10.3390/ma13102227

Horvat, B., Ducman, V., 2019. Potential of Green Ceramics Waste for Alkali Activated Foams 30.

Marvila, M.T., Azevedo, A.R.G. de, Vieira, C.M.F., 2021. Reaction mechanisms of alkali-activated materials. Rev. IBRACON Estrut. Mater. 14, e14309. https://doi.org/10.1590/s1983-41952021000300009

Pacheco-Torgal, F., Castro-Gomes, J., Jalali, S., 2008. Alkali-activated binders: A review. Part 2. About materials and binders manufacture. Construction and Building Materials 22, 1315–1322. https://doi.org/10.1016/j.conbuildmat.2007.03.019

Provis, J., 2013. Alkali activated materials: state-of-the-art report, RILEM TC 224-AAM. Springer, New York.

Rincón Romero, A., Toniolo, N., Boccaccini, A., Bernardo, E., 2019. Glass-Ceramic Foams from 'Weak Alkali Activation' and Gel-Casting of Waste Glass/Fly Ash Mixtures. Materials 12, 588. https://doi.org/10.3390/ma12040588

Škvára, F., 2007. Alkali Activated Material - Geopolymer 16.

Tokoro, C., Suzuki, S., Haraguchi, D., Izawa, S., 2014. Silicate Removal in Aluminum Hydroxide Co-Precipitation Process. Materials 7, 1084–1096. https://doi.org/10.3390/ma7021084

Wei, Y.-L., Cheng, S.-H., Ko, G.-W., 2016. Effect of waste glass addition on lightweight aggregates prepared from F-class coal fly ash. Construction and Building Materials 112, 773–782. https://doi.org/10.1016/j.conbuildmat.2016.02.147